The Airflow Characteristics of Ventilated Cavities in Screen-Type Enclosure Wall Systems (RP-1091)

Joseph P. Piñon
Student Member ASHRAE

Danko Davidovic

Eric F.P. Burnett, Ph.D., P.E.

Jelena Srebric, Ph.D.
Member ASHRAE

ABSTRACT

Many wall systems in North America incorporate a drained and vented air cavity behind the cladding. One important function of this air cavity is to provide a chamber for convective airflow. This ventilation airflow, driven by wind pressure or natural buoyancy, or both, helps to remove moisture from the wall system and, therefore, to dry it. However, there is little conclusive research on the nature and quantity of the cavity airflow behind different screen-type claddings with different venting strategies and cavity depths.

This paper describes a series of experiments using an airflow chamber to investigate and quantify the airflow characteristics in ventilated wall cavities with different cavity depths, vent dimensions, and cladding surfaces, including Plexiglas, brick veneer, and vinyl siding. Vent and cavity depths were limited, for the most part, to sizes and types that are commonly used in residential construction. Realistic predictions of the nature and extent of airflow behind various ventilated cladding designs under specific certain realistic driving forces are given. CFD modeling has been used to obtain information about the nature of the airflow in ventilated cavities. An attempt has been made to provide wall enclosure designers with guidelines concerning ventilated wall cavity design. The results have also been compared to predictions of various analytical expressions for pressure loss through vents, ducts, and cracks.

INTRODUCTION

BACKGROUND

In North America, most of the above-grade enclosure wall systems—especially those used in low-rise residential construction—are screen-type, drained, insulated, and framed systems. Because use of a screen-type cladding inherently acknowledges that water will be transmitted across the screen, it is customary to provide a cavity or air space behind the screen. From this point on, screened and drained enclosure wall systems that are also ventilated are referred to as VSWS (ventilated screen-type wall systems). Figure 1 shows typical components of the outer portion of an idealized VSWS designed with a ventilation chamber. The rectangular vents shown in Figure 1 are similar to open head joints typically used in brick veneer construction.

In addition to the discrete vents shown in Figure 1, other possible venting strategies include horizontal or vertical slots used in panelized curtain walls or precast concrete claddings. Other wall systems, such as contact-applied, vinyl- and wood-based siding systems, may not have any intentional vents or even a ventilation chamber, but they still allow a certain amount of airflow behind the cladding due to joints, spaces, and other holes in the cladding.

Four basic reasons for providing this internal air chamber are (Straube and Burnett 1995) that it provides:

- a capillary break for penetrant rainwater,
- a clear path for gravity drainage,
- an air pressure chamber for screen pressure moderation, and
- a ventilation chamber for convective air movement and moisture control.

Joseph P. Piñon and **Danko Davidovic** are research assistants in the Department of Architectural Engineering, **Eric F.P. Burnett** is a professor in the Departments of Civil and Architectural Engineering and director of research for the Pennsylvania Housing Research Center, and **Jelena Srebric** is an assistant professor in the Department of Architectural Engineering, Pennsylvania State University, University Park, Pa.

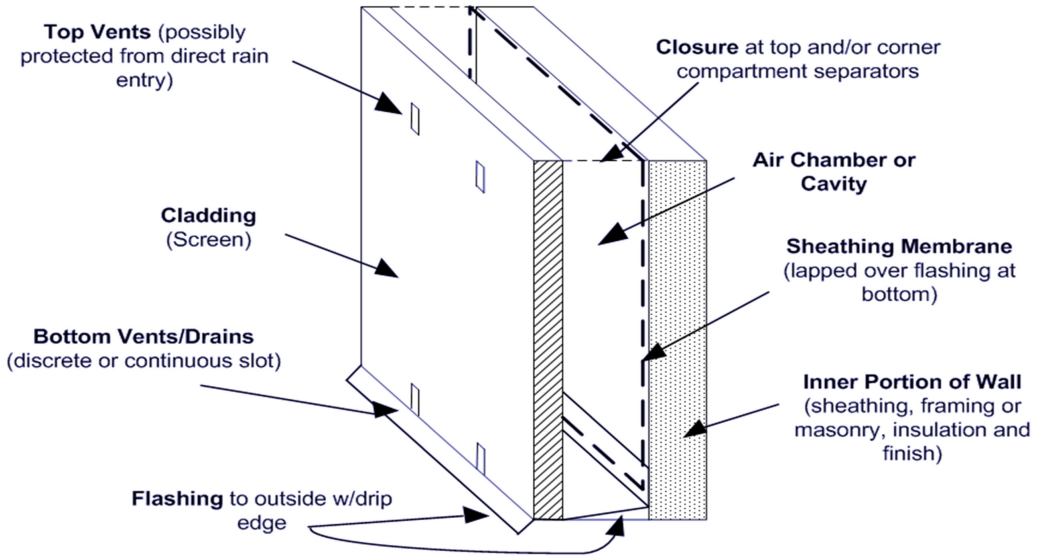

Figure 1 *Components of an idealized ventilated screen-type wall system (VSWS).*

Theoretically, ventilating the air space behind the screen-type cladding with the exterior air offers two additional benefits:

1. The flow of relatively dry outside air—especially in winter—promotes the displacement of moist air and, thus, the drying of the inside face of the cladding and the outside face of the wall layer facing into the cavity.

2. Water vapor diffusing through the inner wall layers can bypass the vapor diffusion resistance of the cladding and can be carried directly to the outside of the wall system.

Thus, ventilation has, in theory, the ability to increase the drying potential of screen-type, drained and ventilated wall systems, especially in assemblies that either store significant amounts of water in the cladding or have a cladding with high vapor resistance. Testing by researchers both in Europe and North America has, to some degree but not conclusively, confirmed the benefits of providing ventilation in screened and drained wall systems (Straube et al. 2004).

In VSWS, one or a combination of two natural forces drives the ventilation air through the air cavity: wind-induced air pressure differentials and thermal and moisture buoyancy (stack effect). The direction of airflow through the air cavity could be from the lower vents to the upper vents or reversed, depending on the combination of the driving forces. Bear in mind that lateral airflow due to wind also occurs and, in some wall systems, may be dominant—for example, contact-applied horizontal vinyl siding.

Despite the theoretical advantages of ventilation drying that, to some extent, have been substantiated by field tests (Straube et al. 2004), there are a number of concerns that need to be addressed. Methods of quantifying or modeling the airflow characteristics of various VSWS have yet to be developed and accepted. These airflow characteristics include:

- pressure losses (resistance to airflow) of the various components of the VSWS and
- the nature of the airflow within wall cavities (velocity profiles and flow regimes).

Five different zones of pressure loss can be identified for a given VSWS: the inlet and outlet vents, the transitions from horizontal to vertical flow (i.e., the bottom and top elbows), and the friction in the cavity. Very few studies are available for accurately predicting the pressure losses of various vents, elbows, and cavities for the typical in-service flow rates experienced by VSWS. Additional complications in modeling the airflow characteristics of VSWS include:

- partially blocked cavities and/or vents (due, say, to mortar droppings),
- vent inserts (usually intended as insect screens),
- irregular shape of most claddings (laps of vinyl and wood siding, roughness of brick, etc.), and
- complex coupling of the five components (inlet and outlet vents, elbows, and cavity).

Objective

The main objective of the work reported here was to study the nature of ventilation airflow in wall systems and to develop the means to model and quantify airflow. As a result, designers should be able to make realistic predictions about the nature and quantity of airflow behind the cladding in ventilated, screened, and drained wall systems (VSWS). This estimate has to be relatively accurate and the procedure reasonably easy for use.

Scope

Both experimental and analytical work was done. The focus was one-story high, ventilated residential wall systems. While the study was mainly directed at residential buildings, the results are relevant for all enclosure wall systems. Only the airflow characteristics are considered—not the resulting impact on drying.

Approach

The airflow characteristics of VSWS are discussed sequentially under the following three headings:

1. CFD modeling
2. Experimental modeling
3. Analytical methodology

CFD MODELING

Computational fluid dynamics (CFD) has become a powerful tool for many engineering applications. Many problems in fluid mechanics and heat transfer have been successfully solved using CFD analyses. For example, an investigation has been done using CFD for the simulation of screen pressure equalization in VSWS (Baskaran 1994). The purpose of modeling the airflow in the ventilated cavities in VSWS was to obtain information about the nature of this airflow.

The commercial CFD software (CHAM 2003) was used. The equations for conservation of mass, momentum (Navier-Stokes equations), and energy are solved in the numerical model using the Reynolds Averaged Navier-Stokes (RANS) equations combined with an algebraic turbulence model (Agonafer et al. 1996). The basic descriptions of the discretized models for the equations of conservation of mass, momentum, energy, and concentration, and algorithms for the solution of the discretized set of equations, are available in the literature (Ferziger and Peric 2002; Patankar 1980; Srebric 2000; Versteeg and Malalasekera 1995). The LVEL turbulence model is chosen as the most appropriate for the simulation of airflow in VSWS. This model is suitable for the conjugate heat transfer problems with low Reynolds numbers. The local Reynolds number is defined based on the local velocity and distance to the closest wall surface in the flow domain.

The boundary conditions are prescribed for the inlet opening in terms of the inlet velocity magnitude and direction. The outlet openings are defined relative to the ambient atmospheric pressure with zero gradients of the velocity and temperature. No-slip condition was assumed on all walls of the ventilated chamber as a boundary condition. For reasons of simplicity and given the similarity with conditions that prevailed during the experiments, only isothermal cases were considered, with driving flow rates in the range that are most likely to occur in VSWS caused by thermal buoyancy only.

Numerical Simulation of Airflow in VSWS

Simulations were run for different vent strategies and different flow rates to complement the sets of experiments with various claddings performed in the BeTL (Building Enclosure Test Laboratory) facility at Pennsylvania State University. The test specimen represents the outer portion of a typical, one-story-high enclosure wall assembly, 4 ft (1.22 m) wide by 8 ft (2.44 m) high.

Only a limited number of representative cases from the experimental program were chosen for simulation. These test series were as follows:

- ***Series 1:*** Four tests involving a 3/4 in. (19 mm) cavity depth with a single, masonry-type weep hole vent opening top and bottom and flow rates of 0.2, 0.6, 1.0, and 4.0 L/s.
- ***Series 2:*** Two tests, one involving a 3/8 in. (19 mm) and the other a 2 in. (50 mm) cavity depth. Each wall panel had two masonry-type weep hole vent openings at the top and bottom and a fixed flow rate of 0.6 L/s.
- ***Series 3:*** Two tests as for Series 2, but with a three weep hole vent configuration.
- ***Series 4:*** Three tests with slot vents and a fixed flow rate of 3.2 L/s. Two tests were done for a 3/8 in. (10 mm) high slot, and one was done for a 3/4 in. (19 mm) high slot vent, using cavity depths of 3/4 in. (19 mm) and 2 in. (50 mm).
- ***Series 5:*** Three tests on test panels 2, 4, and 8 ft wide (600, 1200, and 2400 mm) with two, four, and six weep hole vents at top and bottom, each for a flow rate of 0.31, 0.60, and 1.21 L/s, the same flow velocity in each case.

Space limitations permit discussion of only a few representative situations in this paper; for more information refer to Piñon et al. (2004).

Flow Rate. The two extreme cases from series 1, i.e., constant flow rates of 0.2 and 4.0 L/s, are shown in Figures 2 and 3. Comparison of the velocity fields in Figures 2 and 3 reveals several interesting features about flow through the ventilated wall chambers with single weep hole vents at the top and bottom. The first feature is a nonuniform velocity field vent and the existence of a stagnant zone in the vicinity of the inlet. These stagnant zones are undesirable because the convective drying of that portion of the wall cavity is negligible. The stagnation occurs because the air jet stream coming from the inlet vent hits the back wall and splits into two separate airstreams. Ideally, its momentum is divided into two equal streams of lateral flow at the wall of the ventilated chamber. As the flow rate increases, these divided flow streams have a greater influence on the airflow in the chamber. Along the side walls of the ventilated chamber, eddy zones that are relatively large form in the center regions above the inlet vent. The position and the size of the recirculation zones depend on the flow rate. These two recirculation zones produce stagnant

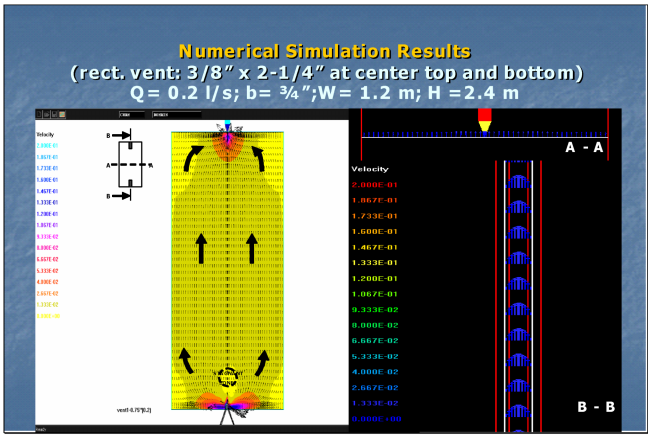

Figure 2 *Velocity field in the middle of cavity space of ventilated chamber for* Q = *0.2 L/s and* b = *19 mm (3/4 in.).*

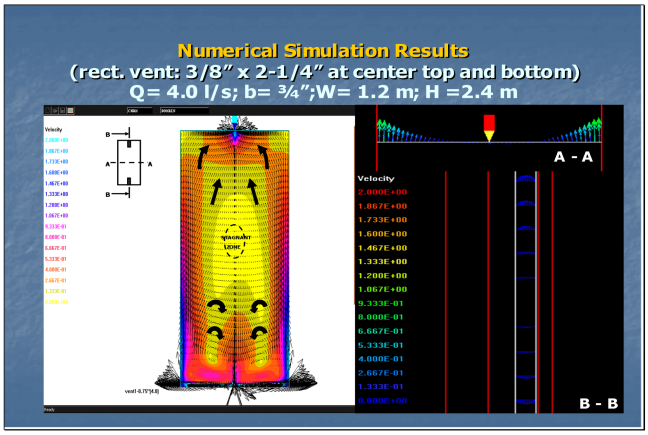

Figure 3 *Velocity field in the middle of cavity space of ventilated chamber for* Q = *4.0 L/s and* b = *19 mm (3/4 in.).*

zones circled in Figures 2, 3, and 4 with dashed lines. The size, shape, and location of this stagnant zone varies with the flow rate. With the increase of the flow rate, the size of the stagnant air zone increases while its position moves upward.

The influence of the side walls on the velocity profile across the width of the ventilated chamber is negligible for the low flow rate regime of less than 1 L/s. When the flow rate is increased, the side stream flows cause significant change, so much that at the mid-height of the panel for 4 L/s, the flow regime is neither uniform nor laminar. Downward mean flow is noticed in the center lower region of the ventilated chamber.

Considering the fact that the maximum flow rate that can be generated by natural buoyancy is less than 1 L/s, these simulations clearly showed that for the lower flow rates, the following applies:

- Along the height and across the width of the vertical flow chamber, the flow stream is mostly uniform.
- Across the depth of the flow chamber, flow could be considered close to uniform.
- Therefore, most of the chamber volume has steady and laminar flow regime.
- The major perturbations are restricted to the vicinity of the inlet and outlet vents.

These are important conclusions and confirm that ventilation analysis can be restricted to laminar flow conditions, at least for natural buoyancy.

Vent Strategy and Cavity Depth. The effect of variation in cavity depth and the number of weep hole vents is shown in Figure 4. Compared to a single vent, it is evident that with two vents the inlet airstream causes less perturbation, and it appears that this perturbation is smaller for the 19 mm cavity depth than for the deeper 50 mm cavity (Piñon et al. 2004).

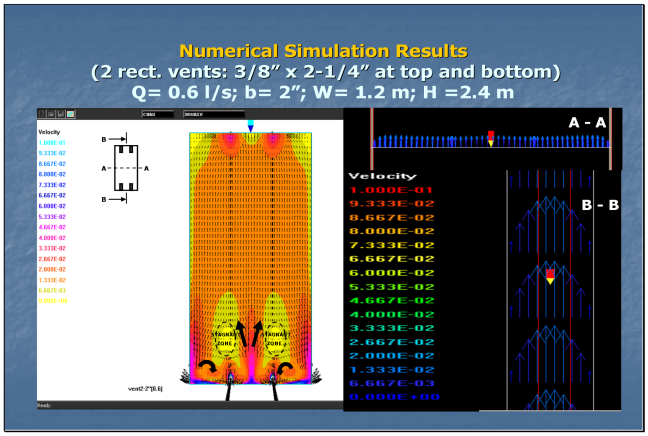

Figure 4 *Velocity field in the middle of cavity space of ventilated chamber for* Q = *0.60 L/s and* b = *50 mm (2 in.).*

From Series 4 simulations, it was evident that with slot vents across the width at the top and bottom of a wall cavity, there is much less resistance and pressure loss than with arrangements of a single discrete vent. Slot vents can accommodate much greater flow rates. The recirculation eddy zones, which are a characteristic of single vents, are avoided. Fully developed laminar velocity profile prevails across nearly the entire height and width of the ventilated chamber. The velocity profile is uniform across the cavity width for the largest part of the ventilated chamber. With slot vents, the variation in velocity across the depth of the chamber is parabolic, confirming the assumption of laminar flow.

Table 1. Parametric Variables Tested

Parameters	Nature and Size		Comments
Cavity depth: Plexiglas and brick panels	3/4 in.	19 mm	
	2 in.	50.8 mm	
	4 in.	101.6 mm	
Cavity depth: Vinyl panels	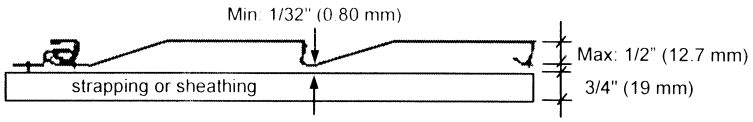		
Type of cladding (or screen)	Plexiglas plate	Smooth	Mortar protrusions in brick cavities
	Brick veneer	Rough	
	Vinyl siding	Nonrectangular + flexible	
Venting strategy (top and bottom)	Slot	3/8 in. (9.5 mm)	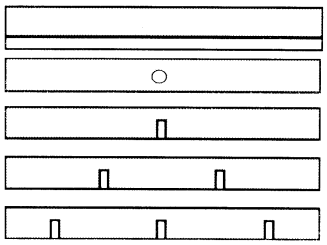
	Slot	3/4 in. (19 mm)	
	Circular hole	Circular (d = 1-1/16 in.) (d = 27.0 mm)	
	One rect. hole	3/8 in. × 2-1/4 in. (9.5 mm × 57.2 mm)	
	Two rect. holes		
	Three rect. holes		
Flow rate range	0.20 L/s – 5.0 L/s	Discrete vents	Based on driving pressures from 0 to 10 Pa.
	1.6 L/s – 20 L/s	Slot vents and vinyl	

EXPERIMENTAL MODELING

Experimental Setup

VSWS test panels with various cavity depths, venting arrangements, and cladding types were built and instrumented. The characteristics of steady-state, induced airflow were studied. Over 180 tests were conducted (each test representing one wall panel tested at a specific flow rate). Table 1 lists the variables that were tested.

For contact-applied horizontal vinyl siding, the minimum cavity depth was 1/32 in. (0.8 mm), which is the slack provided for thermal movement. For contact-applied vertical vinyl siding, the average cavity depth was 1/2 in. (12.7 mm), which is the nominal depth of the laps. For vinyl siding on vertical strapping, the minimum depth of the cavity was 25/32 in. (19.8 mm), which is the depth of the vertical strapping plus the 1/32 in. (0.8 mm) of slack provided for thermal movement.

The slot vents represent common joint widths used in precast screen-type wall systems that utilize an open-jointed venting arrangement. The discrete brick weep hole vents were sized to match standard weep holes used in brick veneer (3/8 in. by 2-1/4 in.), as given by the classification provided by the Brick Industry Association (BIA 1994).

The chosen airflow rate range was based upon preliminary predictions of flow rate given realistic driving forces reported from field tests of 0-10 Pa (Straube and Burnett 1995).

A variable-speed fan (VSD) drives the airflow through the circuit depicted in Figure 5.

1. The intake ambient room air passes through a filter to remove any particulate matter.
2. Airflow proceeds through a flow cart (shown in Figure 6), where it is routed through one of three laminar flow elements (LFE) of different ranges, depending on the desired flow rate. The LFE measures the flow rate.
3. Airflow exits the flow cart into a pressure manifold (shown in Figure 6), which spreads the flow out, straightens the flow, and provides a uniform pressure and flow profile across the bottom vent(s) of the cladding.
4. Airflow enters the bottom entry vent, turns an elbow, proceeds vertically up the cavity, turns another elbow, and is discharged through the top exit vent back into the room air.

Figure 5 also shows the location of the four main static pressure loss measurements. Figure 6 shows all four components of the experimental setup described above. The cladding shown installed in Figure 6 is the Plexiglass panel.

For the brick cladding, real standard bricks were used for the two top and bottom brick courses (so that real rectangular brick weep hole vents could be tested), while the rest of the

brick panel was modeled using an imitation PVC brick panel. The effect of mortar protrusions was also evaluated (see Piñon et al. 2004).

The vinyl siding tested was a common double 4.5 in. (114 mm) Dutch lap profile.

In addition to the four main static pressure loss measurements shown in Figure 5, the following measurements were taken within the cavity: (1) static pressure losses along 11 different portions of the cavity, (2) ten positions of velocity vertically and horizontally, and (3) four positions of temperature and RH.

Table 2 lists the notation used to describe particular tests.

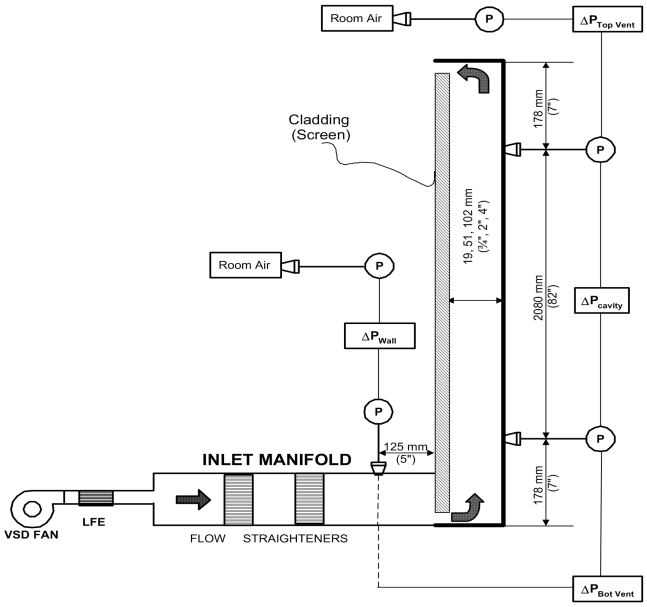

Figure 5 *Airflow circuit and location of four main pressure loss measurements.*

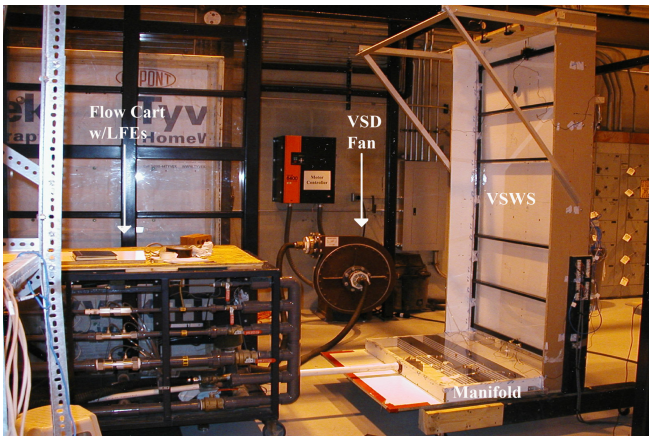

Figure 6 *Experimental setup with Plexiglas panel.*

Table 2. Notation Used to Describe Tests

Parameter	Notation
Cladding	P = Plexiglas B = brick V = vinyl
Cavity depth*	Plexiglas and brick claddings (0.75) = 3/4 in. (19 mm) (2) = 2 in. (50.8 mm) (4) = 4 in. (101.6 mm)
	vinyl cladding (Con) = contact-applied oriented horizontally (ConVert) = contact-applied oriented vertically (S0.75) = 3/4 in. strapping
Venting strategy* (at top and bottom of panel)	Refer to Table 1 for nominal vent dimensions H = one circular hole vent W1 = one rectangular weep hole vent W2 = two rectangular weep hole vents W3 = three rectangular weep hole vents S10 = 3/8 in. (10 mm) slot vent S20 = 3/4 in. (19 mm) slot vent
Flow rates* (L/s)	(0.20) = 0.20 L/s (0.60) = 0.60 L/s (1.00) = 1.00 L/s (1.60) = 1.60 L/s (3.20) = 3.20 L/s (4.0) = 4.0 L/s (5.0) = 5.0 L/s (7.0) = 7.0 L/s (10.0) = 10.0 L/s (15.0) = 15.0 L/s (20.0) = 20.0 L/s
Other descriptors	(M) = 1/4 in. mortar protrusions at joints in brick panel (M0.5) = 1/2 in. mortar protrusions at joints in brick panel
Example	**P(0.75)W1(0.60)** = Plexiglas with 3/4 in. cavity and one rectangular weep hole vent at top and bottom with 0.60 L/s of flow.

Experimental Results

The experimental results discussed here represent the major findings that form the basis for much of the analytical methodology presented later (see Piñon et al. 2004).

- Fitting loss coefficients varied with (1) Reynolds number, (2) cavity depth, and (3) cavity condition.
- Flow disturbance and separation at an inlet sometimes caused recirculation and backflows within the cavity.

Cavity Losses. For most of the panels tested, the measured losses due to friction in the cavity were either zero or negative. The exceptions were for the slot venting arrangements, the brick panels with 1/2 in. (12.7 mm) mortar protrusions, and the vinyl panels. Figure 7 shows the measured cavity losses across various cavity depths and venting strategies when Plexiglas is used as the cladding. Similar results were found for the brick panels without mortar protrusions.

Negative values for friction loss indicate a gain, which was concluded to be due to static regain caused by the expansion of the airflow after the vent. In some cases the flow separation at the vent caused large recirculation zones and backflows (observed by smoke pencils and corroborated by CFD modeling). In all cases, the bottom inlet portions of the cavity showed lower losses than the upper portions of the cavity. In fact, most of the static regain measured can be shown to have occurred between the two lowest cavity pressure measurements. Thus, although Figure 7 shows good agreement between the predicted losses using Darcy-Weisbach and P(0.75)S10 for the flow rates tested, a detailed analysis of the pressure losses along the height of the cavity reveal some interesting behavior. Figure 8 is a revised version of Figure 7, with losses due to friction expressed in terms of Pa/m for a few locations along the height of the cavity for both S10 and S19. S10 clearly shows more disturbance at the vent (due to its smaller width) and, therefore, more subsequent static regain (characteristic of geometric separation). The higher-than-predicted losses for P(0.75)S20 are most likely caused by the dynamic separation of the airflow due to the elbow, which can take up to 50 diameters to settle out (ASHRAE 2001). Bear in mind, however, that the losses of P(0.75)S19 are, as a whole, very minor; therefore, accurate prediction is not critical. For cavity depths below 0.5 in. (12.7 mm) in conjunction with similarly sized slots, cavity losses are expected to dominate any corrections due to the secondary effects discussed.

The nonlinear pressure loss characteristic of brick cavities with mortar protrusions shown in Figure 9 supports the idea that the effect of mortar is best modeled as a fitting loss rather than as an adjustment to the Darcy-Weisbach friction term. The other option would be to adjust the effective depth of the cavity to account for the constriction caused by the protrusion. In reality, a combination of both of these two effects is probably happening: increased friction at the mortar joints and extra losses due to the contraction and expansion of the flow through each mortar joint. However, the Darcy-Weisbach equation shows that frictional losses are proportional to $1/d^3$. Because of this sensitivity, it was not possible to choose a single cavity depth that matched the measured losses well. Therefore, the best way found to model the effect of the 1/2 in.

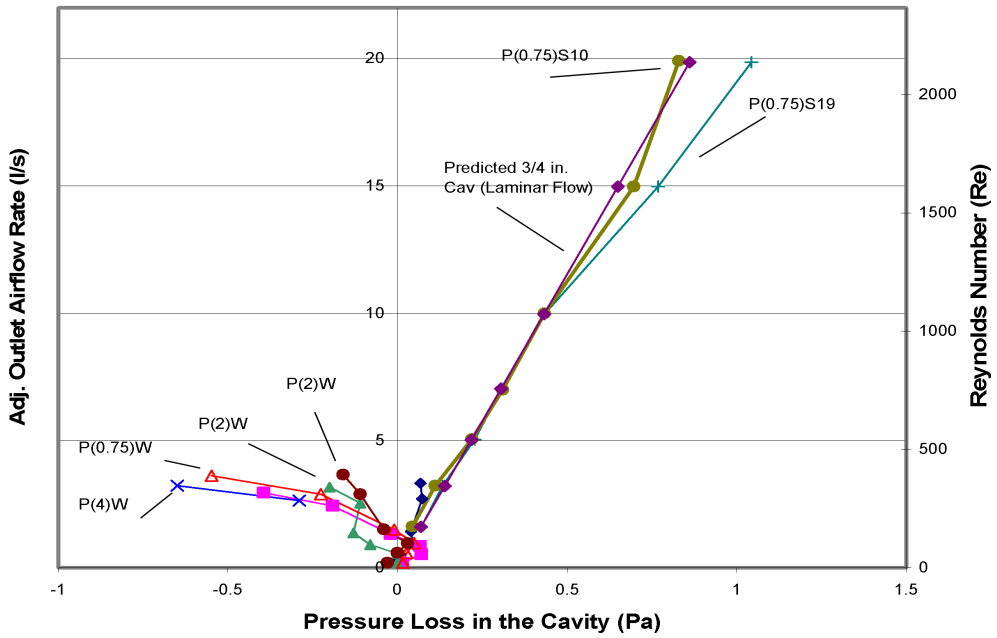

Figure 7 *Friction loss in the cavity for various Plexiglas panels.*

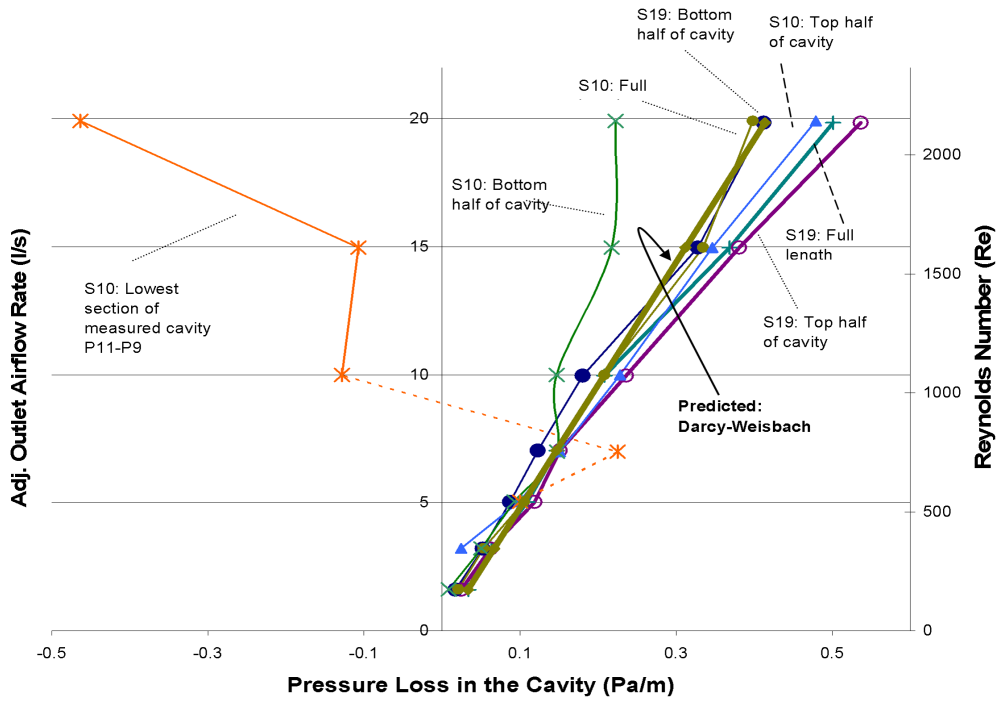

Figure 8 *Friction loss at various lengths in a 3/4 in. (19 mm) cavity.*

(12.7 mm) mortar protrusions of these experiments was to use a fitting loss coefficient.

At one point during testing, a layer of the 1/2 in. (12.7 mm) simulated mortar came loose and constricted the cavity at one point, causing the pressure losses shown in Figure 9 to almost triple in value. This incident underscored the danger that mortar protrusions pose in blocking the cavity and/or vents and thereby eliminating most of the potential ventilation.

Fitting Loss Coefficients. Fitting loss coefficients were calculated from the experimental data for all inlets and outlets for the Plexiglass and brick panels. No attempt was made to subtract the frictional losses along the length of the Plexiglass or brick vents. Therefore, the fitting losses reported here constitute the complete loss of the inlet and outlet insofar as they include any losses due to friction. The flow rate through both inlet and outlet was adjusted for system air leakage by sealing and measuring the air leakage rate in two places: (1) before the inlet and (2) before the outlet. Because of the significant losses due to friction in the cavity for the brick panels with 1/2 in. (12.7 mm) mortar protrusions (M0.5), it was decided to adjust the fitting losses for all of the (M0.5) panels by subtracting the amount of friction that would occur between the pressure measurement points.

Table 3 lists the fitting loss coefficients (including adjusted values where applicable) for all of the Plexiglas and brick panels tested.

The fitting losses reported in Table 3 show the following trends:

- Outlet fitting loss decreases as cavity depth increases.
- Fitting losses through the brick vents are approximately 30% lower than for the Plexiglas vents.
- Mortar in the cavity causes the fitting loss of the inlet in brick vents to decrease by up to 65%.
- The Plexiglas vents exhibit fitting losses about 35% lower than an equivalently sized sharp-edged orifice.
- For discrete Plexiglas vents, the inlet fitting losses are higher than the outlet fitting losses.
- For brick weep hole vents, the inlet fitting losses are lower than the outlet fitting losses.

The complex dependence on vent fitting loss with cavity depth has to do with the complex interaction of the vent-elbow cavity. It was concluded that the mortar in the cavity was acting as "fins," which reduced the amount of backflow, and thereby reduced the overall loss coefficient of the inlet (Piñon et al. 2004).

Modeling a brick vent as a sharp-edge orifice would overestimate its pressure loss by about 80%. This study has shown that, due to their depth ($t/D_h \sim 4.8$), flow through brick vents behaves closer to pipe flow than to sharp-edge orifice flow, meaning that the losses due to entry and exit are similar to pipe behavior for turbulent flow ($C = 0.5$ entrance plus $C = 1.0$ exit equals $C = 1.5$).

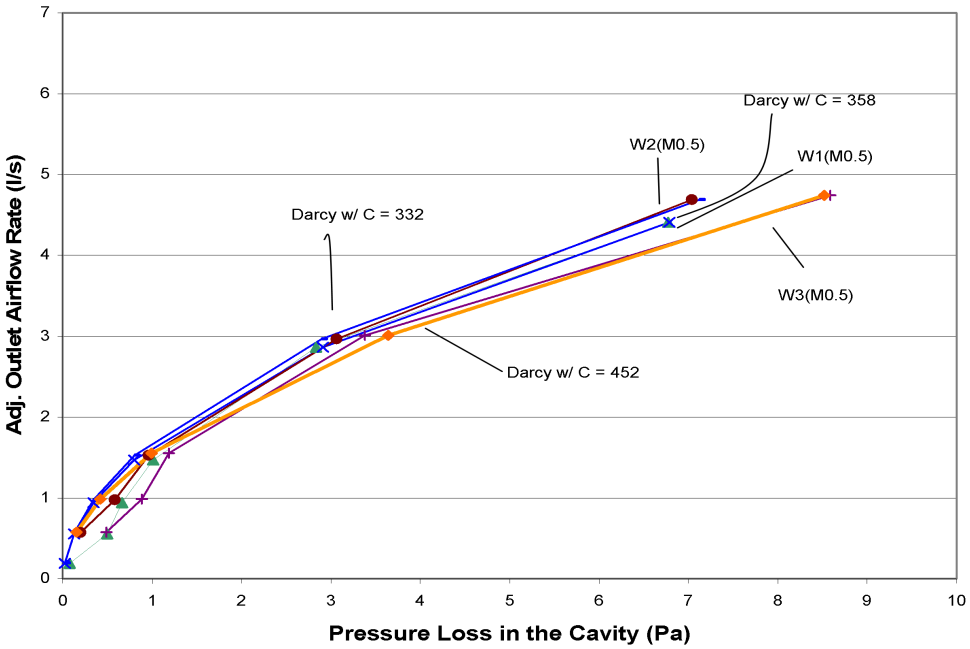

Figure 9 *Modeling effect of mortar protrusions on cavity friction (excluding mortar dams).*

Fitting loss coefficients for entrances, exits, expansions, and other fittings reported in design manuals such as ASHRAE (2001) and SMACNA (1990) are all based upon turbulent flow and commonly found fittings for HVAC design. The main reference that could be found dealing with inlet and outlet losses across the laminar, transitional, and turbulent flow regimes was Idelchik's *Handbook of Hydraulic Resistance* (Idelchik 1994).

Even in Idelchik's work, there is no exact combination of a vent coupled with an expansion into a cavity and an elbow. He does have an equation for calculating fitting loss coefficients in the transition and laminar flow regimes for any edge orifice:

$$C = \zeta_{\varphi} + \bar{\varepsilon}_{0\mathrm{Re}} \cdot \zeta_{0quad} + \lambda(l/D_h) \qquad (1)$$

The ζ_{0quad} term is a fitting loss for the vent for turbulent flow that is based upon the vent dimensions and upon the geometry of the duct sections before and after the vent. For the purposes of comparing the predictions of Equation 1 with the results of this experimental study, the duct sections before and after our inlet and outlets are assumed to be infinite. In addition, the ratio of vent hydraulic diameter to duct hydraulic is assumed to be close to zero, which it is. For those cases, ζ_{0quad} varies from the fitting loss of a sharp-edge orifice (about 2.75) and reduces to 1.50 for deeper orifices. ζ_{0quad} for the 3/16 in. (4.7 mm) thick vents tested in this study is calculated to be 2.75 and, for the 3-5/8 in. (90.5 mm) brick vents, is calculated to be 1.50.

The term $\bar{\varepsilon}_{0\mathrm{Re}}$ is a correction factor to the turbulent flow fitting loss, and for this particular case it goes from about 0.30 to 1.0 as the Reynolds number increases. Similarly, the term ζ_{φ} is an additional correction factor that goes from about 2.0 to 0 as the Reynolds number increases. For this particular case, one would predict that the fitting losses of both brick and Plexiglas would be somewhat lower than those of a sharp-edge orifice. Furthermore, one would expect the fitting losses of the brick vents to be lower than 1.5. The experimental results agree with both of those predictions. The last term of Equation 1 represents the loss due to friction along the sides of the vent. The fitting loss coefficients and total pressure losses calculated using Equation 1 for P(0.75)W1 are shown in Table 4.

The friction factor for the cut Plexiglas is taken from values ASHRAE recommended for PVC as 0.0001 ft. (0.0305 mm). The friction for this case is so small that it is negligible. The friction factors in bold represent the change from laminar friction to transition. As can be seen, use of Idelchik's equation shows that the fitting loss coefficient for either the inlet or the outlet should be around 2.0, which agrees with the experimental results. As can be seen from Figure 10, agreement between predicted and measured pressure losses is within 10% for all but the lowest tested flow rate. Similar agreement was found with the brick vent data; however, it is seen that Idelchik's Equation 1 cannot predict the lower losses through the brick inlets or the dependence of fitting loss on cavity depth and cavity condition (such as mortar).

Vinyl Siding. Application of the standard Darcy-Weisbach expression for friction loss in the cavity modeled the

Table 3. Experimentally Determined Fitting Loss Coefficients

Plexiglas Panel		Fitting Loss Coefficients		
Vent	**Cavity**	**Inlet**	**Outlet**	**Inlet + Outlet**
H	3/4 in.	2.13	2.01	4.14
W1	3/4 in.	2.25	2.02	4.27
	2 in.	2.19	1.38	3.57
	4 in.	2.29	1.19	3.48
W1(2)	3/4 in.	1.99	1.84	3.83
W2	3/4 in.	2.09	1.97	4.06
	2 in.	2.21	1.82	4.03
W3	3/4 in.	1.80	1.58	3.38
	2 in.	1.83	1.44	3.27
S10	3/4 in.	1.81	1.93	3.74
	2 in.	2.24	1.71	3.95
S19	3/4 in.	1.84	3.02	4.86
	2 in.	1.67	2.06	3.73
	4 in.	2.21	2.61	4.82
Brick Panel		**Fitting Loss Coefficients**		
Vent	**Cavity**	**Inlet**	**Outlet**	**Inlet + Outlet**
W1	3/4 in.	1.23	1.54	2.77
(M)		1.16	1.32	2.48
(M0.5)		1.04	1.38	2.42
(M0.5) Adjusted		0.99	1.35	2.34
W2	3/4 in.	1.38	1.65	3.03
(M)		1.29	1.30	2.59
(M0.5)		1.30	1.43	2.73
(M0.5) Adjusted		1.18	1.28	2.46
W3	3/4 in.			
(M)		1.39	1.62	3.01
(M0.5)		1.37	1.76	3.13
(M0.5) Adjusted		0.83	1.54	2.37
Average		1.18	1.45	2.63
*Unadjusted M(0.5) values not included in averages				

Table 4. Fitting Loss Coefficients and Vent Pressure Losses for P(0.75)W1 Calculated Using Idelchik's Equation 1)

Adj. Inlet Flow	V_{vent}		**Friction Factor**	**Friction**			**Fitting Loss Coefficient**	**ΔP**	ΔP_{total} **w/friction**
Q (L/s)	**(m/s)**	**Re**		**(Pa)**	$\bar{\varepsilon}_{0Re}$	ζ_{φ}	**C**	**(Pa)**	**(Pa)**
0.20	0.37	405	0.237	0.006	0.47	0.56	1.84	0.15	0.16
0.56	1.07	1160	0.083	0.017	0.54	0.37	1.85	1.27	1.28
0.92	1.75	1899	**0.054**	0.029	0.58	0.29	1.89	3.46	3.49
1.51	2.85	3098	**0.050**	0.072	0.62	0.24	1.95	9.53	9.60
2.95	5.58	6059	**0.047**	0.257	0.69	0.20	2.08	38.9	39.1
3.74	7.06	7677	**0.046**	0.405	0.71	0.19	2.14	64.0	64.4

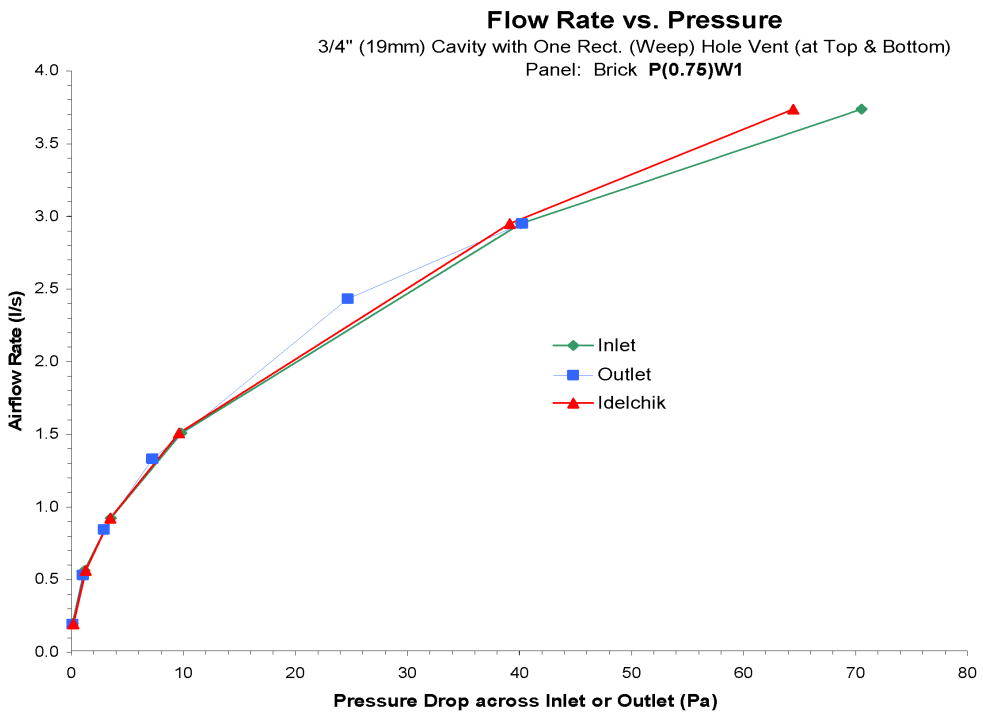

Figure 10 *Comparison of the predictions of Idelchik's (Equation 1) with the measured inlet and outlet losses of* P *(0.75) W1.*

losses in both vinyl on strapping and contact-applied vinyl oriented vertically very well for Reynolds numbers less than 1000. The increase in measured friction in the cavity at higher Reynolds numbers was modeled best using roughness factors for Reynolds numbers of about 1000 and greater (see Figure 11).

For ventilation airflow to occur behind the face of vinyl siding, air has to enter through one of the following: (1) side trim, (2) top trim, or (3) the many lap joints and little weep holes present in the face of vinyl. The purpose of this study of vinyl was to attempt to quantify these resistances so that the relative resistance of each is well understood. Figure 12 is a graph of the adjusted flow rate as a function of the inlet and outlet and through face pressure losses for the three vinyl panels tested.

Analysis of the data shown in Figure 12 leads to the following conclusions:

- There is good agreement between the results of work done at the University of Waterloo (Van Straaten and Straube 2004) (shown in Figure 12 as UW) on the through-face resistance of vinyl and this study.
- The through-face pressure loss characteristics of V(S0.75) are almost identical to V(ConVert) and to the loss characteristics of the starter strip, which makes sense as a starter strip is essentially a combination of a horizontal joint and weep holes.
- The ventilation slots provided by strapping (if left uncovered) allow at least 20 times more flow for a given driving pressure than would occur through the face of vinyl siding. The much lower resistance indicates that most of the flow for vinyl on vertical strapping would be in the vertical direction.

An estimate from Figure 12 shows that it would take about 6 Pa to drive a flow rate of 1 L/s through the face of a 4 ft by 8 ft (1.22 m by 2.44 m) panel of vinyl siding. On the other hand, 6 Pa could drive 1 L/s of flow along the horizontal laps for about 60 meters (Piñon et al. 2004). As the inlet loss at the building edges is about 1 Pa, it can be concluded that for buildings with lengths of less than 50 meters, clad with contact horizontal vinyl siding, the majority of the horizontal ventilation airflow circuits are expected to be in through the corner trim, along the horizontal laps, and out of the opposite corner. Furthermore, the ventilation performance of contact-applied horizontal vinyl systems would be primarily determined by the available horizontal wind pressure gradients.

Velocity Profiles. Velocity was measured at ten different positions along the height and width of the cavity for each flow rate tested. In addition, flow visualization was done for a number of panels using a smoke pencil. Both the measurements and smoke tests confirmed the findings presented in the CFD modeling, i.e., disturbance due to discrete vents, recirculation zones, and backflows. The velocity profiles for many of the panels were highly nonuniform due to the disturbance and flow separation at the inlet; nevertheless, averages of five velocity measurements across the mid-height of the

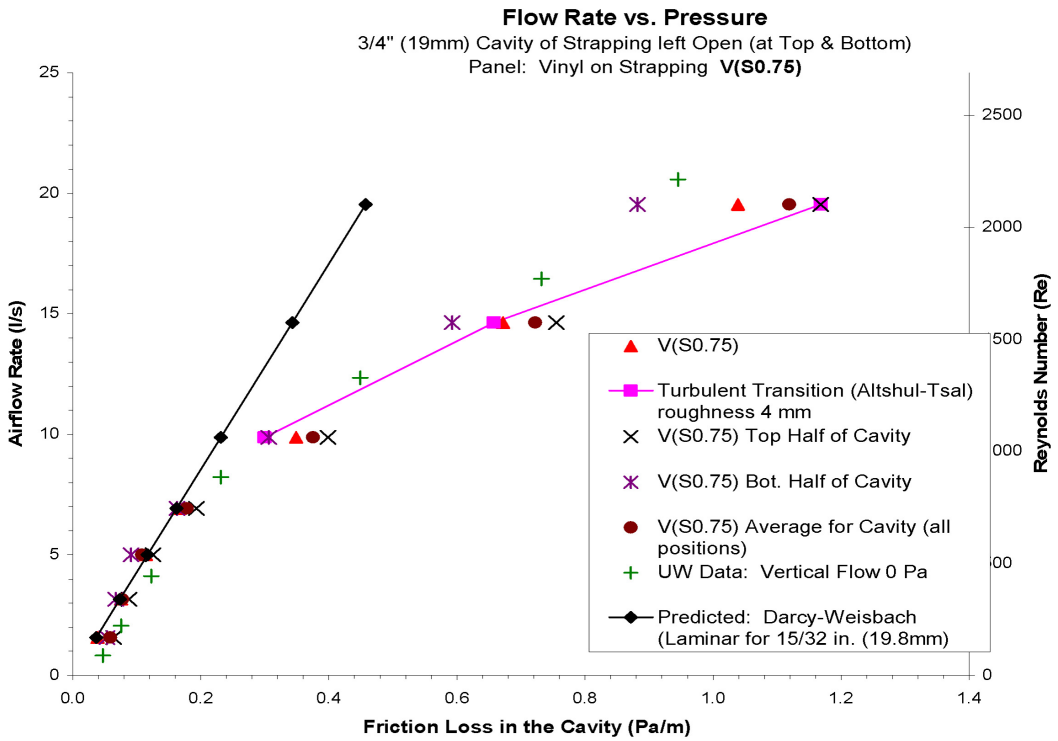

Figure 11 *Friction loss at various lengths of cavity (Pa/m) for V(S0.75).*

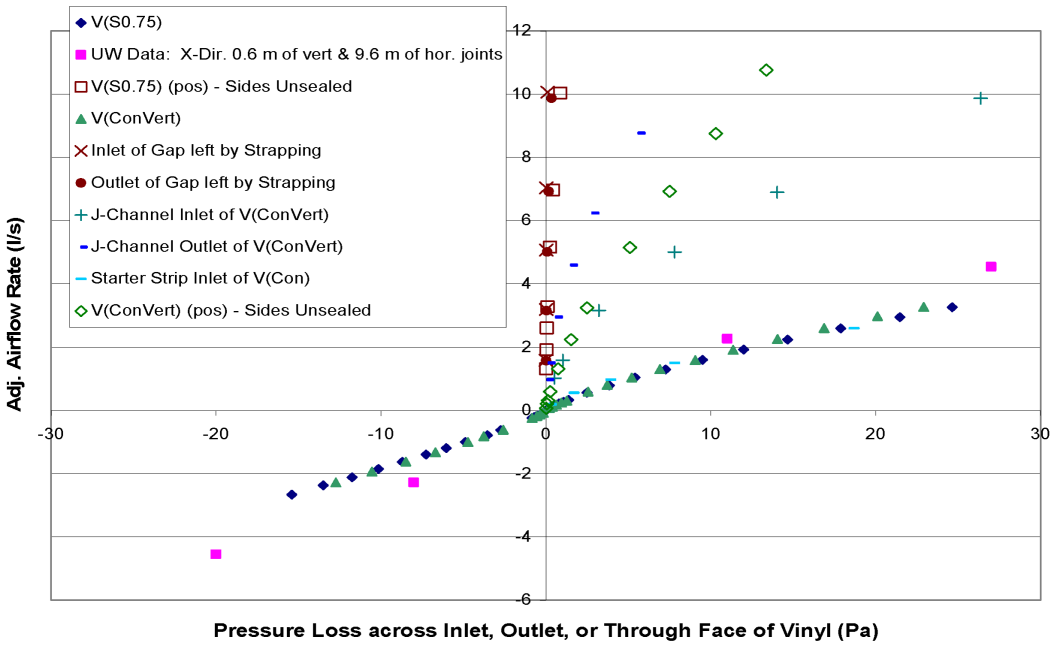

Figure 12 *Pressure losses of inlets and outlets and through face of vinyl.*

cavity almost always fell within the calculated average, and maximum velocities expected for fully developed laminar flow across a variety of both Plexiglas and brick panels tested with a 3/4 in. (19 mm) cavity. Therefore, the average of multiple velocity measurements was concluded to be a reliable indicator of the amount of steady-state induced flow. For a more detailed discussion on the measured velocities, see Piñon et al. (2004).

ANALYTICAL METHODOLOGY

This section presents a methodology for predicting the pressure losses of the components of VSWS. The methodology presented here is based upon an extensive laboratory and theoretical modeling (Piñon et al. 2004) of the pressure losses in VSWS panels.

The standard application of fluid mechanics to HVAC duct design has been shown to provide a good description of the pressure losses in VSWS. For the purposes of VSWS, the HVAC duct design equation for estimating pressure losses can be expressed as shown in Equation 2. See Piñon et al. (2004) and Straube et al. (2004) for a discussion of the units and theory behind each parameter.

$$\Delta P = \frac{\rho}{2} \cdot \left(\frac{f \cdot h}{D_h} \cdot V_{cavity}^2 + \sum (C_{vent} \cdot V_{vent}^2) \right) \quad (2)$$

The experimental results show that the vent-elbow-cavity losses have been shown to be coupled. Because of the complex interaction of flow separation and static regain, it is difficult to separate the pressure losses into separate components. It has been well documented that the disturbances due to closely spaced fittings can interact with each other (Atkin and Shao 2000; Gan and Riffat 1995; Mumma et al. 1997; Shao and Riffat 1995). As reported in ASHRAE, two closely spaced elbows forming a 180-degree turn can exhibit a smaller loss than a single 90-degree bend (ASHRAE 2001). Because these components are always coupled in VSWS, it was of interest to investigate the coupling effects and to recommend simple ways to model the complex behavior. Because the losses were difficult to separate, the pressure losses of the elbows and vents were measured together and referred to as inlets and outlets.

The fitting loss coefficients that have been determined experimentally in this study are referenced to the velocity through the vent. HVAC designers want to know the total pressure loss and then size an appropriate fan for the system. For the design of VSWS, it is more useful to be able to determine, for a given driving pressure, the likely ventilation flow rate. Therefore, it is useful to rearrange Equation 2 in terms of flow rate, as given below in Equation 3.

$$Q = \sqrt{\frac{2\Delta P}{\rho}} \cdot \left(\frac{f \cdot h}{D_h A_{cavity}^2} + \sum \left(\frac{C_{vent}}{A_{vent}^2} \right) \right)^{-\frac{1}{2}} \quad (3)$$

The following equations to determine the friction factors are recommended:

- $f = 96/\mathrm{Re}$ for Reynolds numbers less than 1000
- Altshul-Tsal equation, as given in ASHRAE, for Reynolds numbers greater than 1000.

$$f' = 0.11 \cdot \left(\frac{12 \cdot \varepsilon}{D_h} + \frac{68}{\mathrm{Re}} \right)^{0.25} \quad (4)$$

where

$$\text{if } f' \geq 0.018: f = f'$$

$$\text{if } f' < 0.018: f = 0.85f' + 0.0028$$

For brick cavities containing mortar protrusions larger than half the depth, the addition of an extra fitting loss coefficient referenced to the cavity velocity is recommended. Equation 3 would then become

$$Q = \sqrt{\frac{2\Delta P}{\rho}} \cdot \left(\frac{f \cdot h}{D_h A_{cavity}^2} + \sum \left(\frac{C_{mortar}}{A_{cavity}^2} \right) + \sum \left(\frac{C_{vent}}{A_{vent}^2} \right) \right)^{-\frac{1}{2}}. \quad (5)$$

For those VSWS where cavity friction is negligible, Equations 3 reduces to

$$Q = \sqrt{\frac{2 \cdot \Delta P}{\rho} \cdot \sum \left(\frac{A_{vent}^2}{C_{vent}} \right)}. \quad (6)$$

For the case where the vent areas (inlets and outlets) are identical, Equation 6 reduces to

$$Q = \sqrt{\frac{2 \cdot \Delta P \cdot A_{vent}^2}{\rho \cdot (\sum C_{vent})}}. \quad (7)$$

Table 5 lists the recommended fitting loss coefficients for some typical VSWS vents. These fitting loss coefficients have been determined to be conservative when used in conjunction with cavities 3/4 in. (19 mm) and larger. Recommendations concerning cavity friction losses and use of appropriate roughness factors, etc., are summarized in Table 6.

It was determined that large wall panels could be analyzed as smaller panels with the width determined by the center-to-center distance between vents. If multiple vents are provided in smaller, compartmentalized panels, the same loss coefficient recommended in Table 5 should be used, but the total inlet or outlet area should be used with Equations 3 or 5.

As the venting area for vinyl edge trim (J-channel) was not known in detail, the fitting loss coefficient reported is in terms of an effective air leakage area, as described in ASHRAE (2001).

The fitting loss coefficient for brick vent inserts (insect screens) reported in Table 6 are based upon experimental data reported in Straube and Burnett (1995). The fitting loss coefficient for the inserts should be used in conjunction with the

Table 5. Recommended Fitting Loss Coefficients for Typical VSWS Vents

Vent Type (Non-Rounded or Beveled Edges)	Venting Strategy	Fitting Loss Coefficients	
		Inlet	Outlet
Sharp-edged-orifices	Discrete vents	2.70	2.70
Thin vents (or claddings): $0.15 > t/D_h > 1.2$	Discrete vents	2.0	2.0
	Slot vents 3/8 in. (9.5 mm)	Ignore*	Ignore*
Brick or thick vents: $t/D_h > 1.2$	Discrete vents	1.5	1.5
	w/insect screens	660	660
Vinyl J-Channel	Consider as a slot vent	2.7 w/ EALA of 0.00193 m^2/m	2.7 w/ EALA of 0.00388 m^2/m

* means the pressure loss is negligible
EALA = Effective Air Leakage Area

Table 6. Recommended Procedure for Modeling Cavities Losses

Cladding Type	Venting Strategy	Chamber Depth or Condition	Roughness (ε) or Chamber Fitting Loss	Equation(s) to Use
Smooth, flat cladding (e.g., metal panels, etc.)	Discrete	3/4 in. (19 mm)	Ignore*	Ignore*
	Slot	3/4 in. (19 mm)	Ignore*	3
Brick veneer w/air chamber width 3/4 in. (19 mm)	Weep holes	No mortar protrusions	Ignore*	6 or 7
		Mortar dams < half chamber depth	Ignore*	6 or 7
		Mortar dams > half chamber depth	C_{cav}= 350	5
		Mortar dams full chamber depth	C_{cav}= 1000	5 but try to avoid!
Vinyl siding on 3/4 in. (19 mm) vertical strapping	Chamber left open		Ignore*	Ignore*
Vinyl siding: contact applied- horizontal	Little likely vertical flows; evaluate horizontal losses as contact applied – vertical (see row below)			
Vinyl siding: contact applied- vertical	J-Channel or other trim	Measured as nominal depth of lap	ε = 2.5 mm	3

* means the pressure loss is negligible

full open area of the vent (without insert). The high fitting loss coefficient of the vent inserts shows that they restrict the flow of air to about 5% of that of an unobstructed vent.

The effect of brick-vent inserts and cavity depths smaller than 3/4 in. (19 mm) on ventilation potential still needs to be investigated.

SUMMARY AND DISCUSSION

The airflow characteristics of VSWS have been studied using analytical, numerical, and experimental simulation. This comprehensive study has resulted in a number of conclusions and recommendations, such as:

1. How to model various wall cavity sizes and conditions.
2. Experimentally derived fitting loss coefficients of various venting strategies.
3. Use of point velocity measurements to predict steady-state induced flow.
4. Qualitative agreement with a CFD model of VSWS.

Measurements revealed that modeling brick vents as sharp-edged orifices would overestimate their expected pressure losses by about 80%. Use of one of Idelchik's equations has been shown to provide good prediction of the fitting loss coefficients for a few vents. However, it is clear that the equation cannot predict the variability measured in these tests across cavity depths, between the inlet and outlet, and the

lower fitting losses due to protrusions in the cavity. But Idelchik's equations are the best expressions available in the literature for estimating vent losses at the low flow regimes. Until further analysis is done, it is recommended to use the experimentally derived fitting losses reported from this study.

The CFD modeling confirmed that, for the range of flow rates likely to be produced by natural buoyancy, the nature of flow within the ventilation chamber is essentially fully developed laminar flow. Nonlaminar flow and perturbation may be confined to the vent regions, and the greater the number of discrete vents, the less this influence is likely to be. The general characteristics of the flow of air in VSWS have been captured by CFD analysis.

ACKNOWLEDGMENTS

This study was the result of cooperative research (RP-1091) between the American Society of Heating, Refrigerating and Air-Conditioning Engineers, Inc. (ASHRAE), the Pennsylvania Housing Research Center (PHRC) at Pennsylvania State University (PSU), the Building Engineering Group (BEG) at the University of Waterloo (UW), and Oak Ridge National Laboratory (ORNL).

REFERENCES

Agonafer, D., L. Gan-Li, and D.B. Spalding. 1996. LVEL turbulence model for conjugate heat transfer at low Reynolds numbers. American Society of Mechanical Engineers, EEP, Vol. 18, Application of CAE/CAD to Electronic Systems, pp. 23-26.

ASHRAE. 2001. *2001 ASHRAE Handbook—Fundamentals*. Atlanta: American Society of Heating, Refrigerating and Air-Conditioning Engineers, Inc.

ASHRAE. 1999. *ASHRAE Standard 120P, Method of Testing to Determine Flow Resistance of HVAC Ducts and Fittings*. Atlanta: American Society of Heating, Refrigerating and Air-Conditioning Engineers, Inc.

Atkin, S.M., and L. Shao. 2000. Effect on pressure loss of separation and orientation of closely coupled HVAC duct fittings. *CIBSE A: Building Serv. Eng. Res. Technol.* 21(3):175-178.

Baskaran, A. 1994. A numerical model to evaluate the performance of pressure equalized rainscreen walls. *Building and Environment* 29(2):159-171.

BIA. 1994. Brick masonry rainscreen walls: Technical Note on brick construction: #27. Reston, Va.: Brick Industry Association.

CHAM. 2003. POLIS—Encyclopaedia. PHOENICS Commercial Software Manual, UK.

Ferziger, J.H., and M. Peric. 2002. *Computational Methods for Fluid Dynamics*, 3d ed. Springer-Verlag, Berlin, New York.

Gan, G., and S.B. Riffat. 1995. K-factors for HVAC ducts: Numerical and experimental determination. *Building Serv. Eng. Res. Technol.* 16(3):133-139.

Idelchik, I.E. 1994. *Handbook of Hydraulic Resistance*, 3d edition. Boca Raton, Fla.: CRC Press.

Mumma, S., T. Mahank, and Yu-Pei Ke. 1997. Close coupled ductwork fitting pressure drop. *HVAC&R* 3(2):158-177.

Patankar, S.V. 1980. *Numerical Heat Transfer and Fluid Flow*. New York: Hemisphere Publishing Corp.

Piñon J., D. Davidovic, E. Burnett, and J. Srebric. 2004. ASHRAE 1091-Report #5. Characterization of ventilation airflow in screened wall systems. The Pennsylvania Housing Research/Resource Center. Pennsylvania State University.

Shao, L., and S.B. Riffat. 1995. Accuracy of CFD for predicting pressure losses in HVAC duct fittings. *Applied Energy* 51(1995):233-248. Elsevier Science, Ltd.

SMACNA. 1990. *HVAC Systems Duct Design*, 3d edition. Sheet Metal and Air Conditioning Contractors' National Association, Inc., Chantilly, Va.

Srebric, J. 2000. Simplified methodology for indoor environment design. Ph.D. thesis, Massachusetts Institute of Technology, Boston, Mass.

Straube, J., R. VanStraaten, E. Burnett, and C. Schumacher. 2004. ASHRAE 1091-Report #1. Ventilated wall systems: Review of literature and theory. The Building Engineering Group. University of Waterloo.

Straube, J., and E. Burnett. 1995. Vents, ventilation drying, and pressure moderation. Building Engineering Group (University of Waterloo) report for the *CMHC*, Dec.

Van Straaten, R., and J. Straube. 2004. Laboratory study of ventilation airflows in vinyl siding—Draft Final Report. *ASHRAE 1091 – Report #4.*

Versteeg, H.K., and W. Malalasakera. 1995. *A*n introduction to computational fluid dynamics—The finite volume method. Longmans Group Ltd., UK.